Published in final edited form as:
J Proteomics. 2014 September 23; 109: 63–75. doi:10.1016/j.jprot.2014.06.010.

Quantitative Phosphoproteomics Reveals Novel Phosphorylation Events in Insulin Signaling Regulated by Protein Phosphatase 1 Regulatory Subunit 12A

Xiangmin Zhang[1,#], **Danjun Ma**[1,#], **Michael Caruso**[1], **Monique Lewis**[1], **Yue Qi**[1], and **Zhengping Yi**[1,*]

[1]Department of Pharmaceutical Sciences, College of Pharmacy and Health Sciences, Wayne State University, Detroit, MI, 48202, USA

Abstract

Serine/threonine protein phosphatase 1 regulatory subunit 12A (PPP1R12A) modulates the activity and specificity of the catalytic subunit of protein phosphatase 1, regulating various cellular processes via dephosphorylation. Nonetheless, little is known about phosphorylation events controlled by PPP1R12A in skeletal muscle insulin signaling. Here, we used quantitative phosphoproteomics to generate a global picture of phosphorylation events regulated by PPP1R12A in a L6 skeletal muscle cell line, which were engineered for inducible PPP1R12A knockdown. Phosphoproteomics revealed 3876 phosphorylation sites (620 were novel) in these cells. Furthermore, PPP1R12A knockdown resulted in increased overall phosphorylation in L6 cells at the basal condition, and changed phosphorylation levels for 698 sites (assigned to 295 phosphoproteins) at the basal and/or insulin-stimulated conditions. Pathway analysis on the 295 phosphoproteins revealed multiple significantly enriched pathways related to insulin signaling, such as mTOR signaling and RhoA signaling. Moreover, phosphorylation levels for numerous regulatory sites in these pathways were significantly changed due to PPP1R12A knockdown. These results indicate that PPP1R12A indeed plays a role in skeletal muscle insulin signaling, providing novel insights into the biology of insulin action. This new information may facilitate the

[*]Address reprint requests to: Zhengping Yi, Ph.D., Department of Pharmaceutical Sciences - Room 3146, Eugene Applebaum College of Pharmacy/Health Sciences, Wayne State University, 259 Mack Ave., Detroit, MI 48201, (313) 577-0823, zhengping.yi@wayne.edu.
[#]These authors contribute equally

AUTHOR CONTRIBUTIONS

X.Z. designed and performed biological and proteomic experiments, analyzed data, generated figures, and wrote the manuscript. D.M. designed experiments, analyzed data, and wrote the manuscript. M.C., and M.L., designed experiments and edited the manuscript. Z.Y. supervised the project, designed the biological and proteomic experiments, analyzed data, and wrote the manuscript.

COMPETING FINANCIAL INTERESTS

The authors declare no competing financial interests.

Conflict of Interest

The authors declare no competing financial interests.

design of experiments to better understand mechanisms underlying skeletal muscle insulin resistance and type 2 diabetes.

Keywords

Quantitative phosphoproteomics; serine/threonine protein phosphatase 1 regulatory subunit 12A (PPP1R12A); insulin signaling; protein phosphatase 1 (PP1); skeletal muscle; SILAC

1. Introduction

Protein phosphorylation and dephosphorylation, regulated by kinases and phosphatases respectively, play a central role in a wide variety of biological processes. Skeletal muscle is the major site of insulin-stimulated glucose disposal, and defects in insulin signaling in skeletal muscle are considered to be one of the main causes for a large number of disease conditions, such as insulin resistance, metabolic syndrome, and type 2 diabetes (T2D) [1–7]. Majority of research on the regulation of phosphorylation events in skeletal muscle insulin action has been focused on the role of kinases. However, the mechanisms for serine/threonine phosphatase action in insulin signal transduction is largely unknown.

Serine/threonine protein phosphatase 1 (PP1), an abundant serine/threonine phosphatase, regulates a large variety of cellular processes through protein dephosphorylation events in eukaryotes [8–10]. The catalytic subunit of PP1 (PP1c) is relatively non-specific by itself, and interaction with regulatory subunits is required for its specificity [8–10]. Protein phosphatase 1 regulatory subunit 12A (PPP1R12A), also known as myosin phosphatase target subunit 1 (MYPT1), is widely expressed in various cell types [11]. PPP1R12A whole body knock-out in mice is embryonic lethal [12], and PPP1R12A intestinal smooth muscle specific knock-out mice exhibited abnormal contractile phenotypes, suggesting an critical role in muscle function [13]. PPP1R12 plays important roles in various cellular processes through modulating the activity and specificity of PP1c against several identified protein substrates [11, 14, 15].

One of the well-known functions of PPP1R12A is to form a myosin phosphatase holoenzyme with the δ isoform of PP1c (PP1cδ, also called PP1cβ), thereby modulating the specificity and activity of PP1cδ against phosphorylated myosin, which ultimately regulates muscle contraction and cell migration [11, 14–17]. The PPP1R12A/PP1cδ complex also has been found to dephosphorylate polo-like kinase 1 (PLK1), leading to mitotic arrest [18]. A number of other proteins involved in different biological processes have been shown to interact with PPP1R12A, such as interleukin-16 and telokin, suggesting that PPP1R12A may be involved in various additional cell functions [11, 15, 16]. Recently, we have identified PPP1R12A and PP1cδ as novel endogenous interaction partners with insulin receptor substrate 1 (IRS1) [19]. Inhibitor experiments indicated that the interaction of PPP1R12A and PP1cδ with IRS1 is diminished upon inhibition of Akt and mTOR/Raptor [20]. Moreover, we have demonstrated that insulin stimulates or suppresses multiple phosphorylation sites of PPP1R12A [21]. These results provided the first evidence that PPP1R12A may regulate skeletal muscle insulin action through tuning PP1cδ activity and specificity. Nonetheless, little is known about the phosphorylation events controlled by the

PPP1R12A in the context of skeletal muscle insulin signaling. Moreover, majority of research on the abnormalities of phosphorylation in skeletal muscle insulin action focus a few known phosphorylation targets.

In the present work, we analyzed global protein phosphorylation changes caused by PPP1R12A protein knockdown in L6 cells, a well-established insulin-sensitive rat skeletal muscle cell line, using quantitative phosphoproteomics. We generated the first doxycycline (Dox) inducible PPP1R12A knock-down L6 cell line and used titanium dioxide (TiO_2) beads to enrich phosphopeptides. The enriched phosphopeptides were analyzed by high performance liquid chromatography-electrospray ionization tandem mass spectrometry (HPLC-ESI-MS/MS) using an LTQ-Orbitrap Elite. The goal of the study is to determine whether PPP1R12A, a phosphatase regulatory subunit, indeed regulates multiple phosphorylation events under basal and/or insulin-stimulated conditions in skeletal muscle cells.

2. Material and methods

2.1 Materials

The 293FT cell line, high glucose DMEM media, penicillin-streptomycin-glutamine mixture (PSG), MEM non-essential amino acids solution (NEAA), sodium pyruvate, G418 and Alexa Fluor® 568 goat anti-mouse IgG (H+L) antibody were from Life Technologies. Normal fetal bovine serum (FBS), protease inhibitor cocktail, phosphatase inhibitor cocktails (2 & 3), HPLC grade acetonitrile (ACN), trifluoroacetic acid (TFA) and formic acid (FA) were from Sigma. The dialyzed FBS, $^{13}C_6{}^{15}N_4$ L-arginine, 4,4,5,5-D_4 L-lysine and DMEM media deficient in arginine and lysine were from Thermo Fisher Scientific. Sequence grade trypsin, treated with L-(tosylamido-2-phenyl) ethyl chloromethyl ketone (TPCK), was from Promega. Primary antibody to myosin heavy chain (MF20) was from R&D systems. The PPP1R12A antibody (H-130) was from Santa Cruz. The β-actin antibody was from Cell Signaling. The 40S ribosomal protein S6 (RPS6) antibody was from Santa Cruz. The anti-phospho-RPS6 (S240/244) was from Cell Signaling. The horseradish peroxidase (HRP)-linked donkey anti-rabbit IgG was from GE Healthcare. Plasmids Tet-pLKO-puro (#21915), psPAX2 (#12260), pMD2.G (#12259) were from Addgene. Titanium dioxide (TiO_2) beads were from GL Sciences Inc. (Tokyo, Japan). Amicon Ultra-0.5 Centrifugal Filter Unit with Ultracel-10 membrane (10 kD) was from Millipore.

2.2 Plasmid construction and lentivirus packaging

The oligonucleotides 5′-ccggaccattgtttcatgttaattcaagagattaacatgaaacaatggtcttttt-3′ and 5′-aattaaaaagaccatt gtttcatgttaatctcttgaattaacatgaaacaatggt-3′ were annealed to form dsDNA encoding shRNA sequences targeting the 3′ non-translated sequence (NTS) of rat PPP1R12A mRNAs. The dsDNA sequence was cloned into *Age*I-*Eco*RI digested plasmid Tet-pLKO-puro under the regulation of the inducible hybrid H1 promoter [22]. The resulting plasmids were verified by DNA sequencing. Lentivirus carrying shRNA coding sequence was packaged by cotransfecting 293FT cells with each verified shRNA encoding plasmid, plasmid pMD2.G (encoding VSV-G) and psPAX2 (encoding HIV Gag, Pol, Rev) as described previously [23].

2.3 Cell culture and isotopic metabolic labeling

293FT cells were maintained in DMEM supplemented with 10% FBS, 1% PSG, 1mM sodium pyruvate and 1% NEAA. Rat L6 myoblasts were maintained in growth medium (DMEM with 10% FBS and 1% PSG). Once myoblasts reached confluence, differentiation was induced by maintaining the cells in myotube induction media (DMEM containing 2% FBS and 1% PSG) for 8 days. Stable isotope labeling with amino acids in cell culture (SILAC) [24–26] was used to label L6 myotube cells, which were used as an internal standard for quantification. For isotopic metabolic labeling, newly subcultured L6 cells were transferred into arginine/lysine-free DMEM supplemented with 10% dialyzed FBS, 0.4 mM $^{13}C_6{}^{15}N_4$ L-arginine and 0.8 mM 4,4,5,5-D_4 L-lysine (Thermo Fisher Scientific). L6 myoblasts were expanded in the labeling media for 6 passages to ensure complete labeling, and were induced into myotubes by lowering the concentration of FBS to 2%. The labeled L6 myotubes were serum-starved for 3 hrs, and immediately stimulated by 100 nM insulin for 0 min, 30 min, 60 min and 120 min. The cells were immediately harvested, lysed in 8 M urea containing 4% CHAPS, 40 mM Tris-base, 65 mM DTT, and a mixture of phosphatase and protease inhibitors. The lysate was centrifuged at 15,000 × g for 30 min at 4°C. The supernatants were collected and the protein concentration was determined with Bradford assay. Equal amounts of protein in the four time point were mixed as the “heavy” labeled standard and stored at −80°C for further use.

2.4 Transduction and cell line development

The harvested lentivirus was mixed with polybrene to final concentration of 5 μg/ml and incubated with the L6 myoblasts at 37°C overnight. The transduced cells were further maintained in growth media for 2 days. Then, the myoblasts were trypsinized and 1:10 seeded in growth media containing 700 μg/ml G418 to form separate colonies. The isolated single colonies were expanded and cultured in growth medium containing 100 ng/ml Dox. Western blotting was used to evaluate Dox inducible PPP1R12A knock-down as described in references [19, 20]. The clones shown Dox-inducible PPP1R12A knock-down were further cultured in myotube induction media for 8 days. The cells were fixed by 4% PFA and immunostained with mouse monoclonal anti-MyHC (MF20) and counterstained with DAPI. One of the clones showed efficient Dox-inducible PPP1R12A knock-down and myotubes formation, and was used in phosphoproteomic study.

2.5 Dox induction, cell starvation and insulin stimulation

The confluent myoblasts grown in sixteen 15 cm dishes were maintained in 20 ml of DMEM containing 2% FBS, 1% PSG with or without 100 ng/ml Dox for three days. The half-life of Dox in cell culture medium is approximately 24 hrs. To maintain continuous inducible PPP1R12A knock-down in cell culture, the medium was replaced every day. At the 3rd day, all cells were washed twice with DPBS and starved in 20 ml of DMEM containing 0.2% BSA with or without 100 ng/ml Dox for 4 hrs. At the end of starvation, four dishes of cells from each group were treated without or with 100 nM insulin for 15 min.

2.6 Enrichment of phosphopeptides using TiO_2 beads

Phosphopeptides were enriched using TiO_2 beads after in-solution trypsin digestion of lysate proteins as described in reference [27] with recent modifications. For each sample, the cells were washed with iced-cold DPBS for three times, scraped, and harvested in a 15 ml Falcon tube. The supernatant was removed completely after two times of centrifugations at 1000 rpm, 4°C for 5 min. The cell pellet was lysed in 1.25 ml of 8 M urea containing a mixture of phosphatase and protease inhibitors. After centrifugation at 4°C, 15,000 rpm, 15 min, the cleared supernatants were quantified using Bradford reagent. For each sample, 2.5 mg of total protein was spiked with 0.5 mg of "heavy" labeled ($^{13}C6$ $^{15}N4$ L-arginine, 4,4,5,5-D_4 L-lysine) standard.

Each sample was desalted using an Amicon 10 kD spin column at 14,000 × g, 4°C. The protein pellet in each column was washed twice with 400 μl of 40 mM ammonium bicarbonate (ABC) at 14,000 × g. The washed protein pellet was transferred to a fresh 2 ml collection tube through invert centrifugation at 3,000 × g. Then, each protein pellet was mixed with 200 μl of TPCK-trypsin (15 μg) and subjected to overnight digestion in a 37°C shaker (600 rpm). In the next morning, 200 μl of TPCK-trypsin (15 μg) was supplemented to each dissolved protein sample and for additional 8 hrs of digestion. The resulting peptides solution was filtrated through a fresh 10 kD Amicon column and dried using a Speed-Vac. The TiO_2 beads resuspended in loading buffer (65% ACN, 2% TFA and saturated with glutamic acid) were added to the dried peptides at 1 mg TiO_2 beads per sample. It was then supplemented with the loading buffer to final volume of 500 ul. After gentle rotation at RT for 30 min, the beads were collected through centrifugation at 3000 rpm for 1min. The resulting supernatant was further incubated with TiO_2 beads with the same procedure and the beads were collected. All collected beads were washed with washing buffer I (65% ACN, 0.5% TFA) twice and washing buffer II (65%ACN, 0.1% TFA) twice. The bound peptides were eluted once with elution buffer I (300 mM NH4OH, 50% ACN) and twice with elution buffer II (500 mM NH4OH, 60% ACN). The eluates for each sample were combined and dried using a Speed-Vac. The dried peptides were reconstituted in 0.1% TFA.

2.7 HPLC-ESI-MS/MS analysis

The peptide mixture was separated with a linear gradient of 5–43% buffer B (80% ACN and 0.1% FA) in 180 min at a flow rate of 250 nl/min on a C_{18}-reversed phase column (75 μm ID, 15 cm length) packed in-house with ReproSil-Pur C18-AQ μm resin (Dr. Maisch GmbH) in buffer A (0.1% FA). A nanoflow Easy-nLC system (Thermo Scientific) was on-line coupled to a Thermo Finnigan LTQ-Orbitrap Elite fitted with a nanospray flex Ion source (Thermo Fisher, San Jose, CA).

A "top 15" data-dependent tandem mass spectrometry approach was utilized to identify peptides in the samples. In a top 15 scan protocol, a full scan spectrum (survey scan, 300–1650 Th) is acquired followed by collision-induced dissociation (CID) mass spectra of the 15 most abundant ions in the survey scan. The survey scan was acquired using the Orbitrap mass analyzer to obtain high mass accuracy and high mass resolution data (240,000 resolution), and up to 15 of the most intense peptides were selected and subjected to fragmentation in the linear ion trap (LTQ). Dynamic exclusion was set at 30 seconds. The

charge state rejection function was enabled with “unassigned” and “single” charge states rejected. By knowing the accurate mass and fragmentation pattern of the peptide, the peptide’s amino acid sequence can be reliably inferred.

2.8 Phosphopeptide identification and quantification

Raw MS files were processed using the MaxQuant software [28–31](ver.1.3.0.5) against a database with forward and reversed Uniprot Rat protein sequences, downloaded from www.uniprot.org on 3/6/2013. Standard settings in the MaxQuant were applied. Parent mass tolerance was 5 p.p.m., and fragment mass tolerance was 0.5 Da. Two missing trypsin cleavage site was allowed. Oxidised Methionine (M), phosphorylation (STY) and acetylation (protein N-term) were allowed as a variable modification. The false discovery rate (FDR) for both proteins and peptides (which had to have at least 6 amino acids) was set to 0.01. In addition, only phosphosites with a localization probability greater than 0.75 were considered as identified, a commonly used threshold in phosphoproteome studies [32–34], and these phosphosites were classified as class I phosphosites [32–34].

To be used in comparisons between the two groups of samples, phosphorylation sites need to satisfy the following criteria: 1). Identified in at least 3 out of the 4 samples in one group of the comparison; 2). with a fold change greater than 1.5 (i.e., 1.5 fold increase) or less than 0.66 (i.e., 1.5 fold decrease) between comparisons. The stable-isotope-labeled phosphorylation sites identified in all sixteen samples were chosen as the “universal standard” for normalization to account for the variations in the sample preparation and HPLC-ESI-MS/MS analysis. The total peak area of isotope-labeled phosphopeptides identified in all sixteen samples was calculated for each sample. The normalized peak area for non-labeled phosphosites were calculated by normalizing the peak area of a phosphorylation site (PA*i*) against the total peak area of isotope-labeled phosphorylation sites in all sixteen samples in the same sample:

$$\mathrm{Norm}{:}i=\frac{\mathrm{PA}i}{\mathrm{Sum\ of\ the\ peak\ area\ for\ the\ labeled\ phosphorylation\ sitesidentified\ in\ all\ sixteen\ samples}}$$

The normalized peak area for each phosphosite were compared among the groups to assess effects of PPP1R12A knockdown and/or insulin on phosphorylation levels. Statistical significance was assessed by independent *t*-test. Differences were considered statistically significant at $P < 0.05$.

2.9 Bioinformatics

Pathway analysis on phosphorylated proteins were performed using Ingenuity Pathway Analysis (Ingenuity Systems, Inc., Redwood City, CA; www.ingenuity.com), a popular bioinformatics analysis software package [35–37] that contains biological and chemical interactions and functional annotations created by manual curation of the scientific literature [38, 39].

3.10 Western blot confirmation of phosphorylation site

Western blot confirmation was performed as described previously [19, 20]. Briefly, L6K76 myoblasts with or without 100 ng/ml Dox induction were serum starved for 4 h and treated with or without insulin (100 nM) for 15 min. The cells were lysed and protein concentration was estimated using the Bradford assay. Samples were boiled in SDS-PAGE sample buffer and resolved on 4–15% 1D-SDS-PAGE, transferred onto nitrocellulose membranes (Bio-Rad), and analyzed by Western blot (WB) with the appropriate antibodies, and the immune complex was detected by chemiluminescence.

3. Results

3.1 L6 cell line with Dox-inducible knockdown of PPP1R12A

We designed a shRNA targeting the 3 non-translated sequence (NTS) of rat PPP1R12A mRNAs (referred as PPP1R12A shRNA). The PPP1R12A shRNA was cloned into a Dox-inducible shRNA expressing lentiviral vector Tet-pLKO-puro (Addgene # 21915) under the regulation of the inducible hybrid H1 promoter [22]. By transducing L6 myoblasts with the resulting lentivirus, we successfully selected G418-resistant clones showed efficient PPP1R12A knock-down at 48–72 hrs post addition of Dox. The established clones were maintained in DMEM containing 2% fetal bovine serum (FBS) for 8 days. The cells were examined with mouse monoclonal anti-MyHC (MF20), and showed myotube formation. One L6 clone (referred as L6K76) showed Dox-inducible PPP1R12A knockdown (Fig. 1A, 1B) and can be differentiated into myotubes was chosen as the cell model for this study (Fig. 1C).

3.2 Phosphoproteomic profiling of rat myoblasts

The L6K76 cells were grown until 100% confluence, and subjected to Dox-inducible PPP1R12A knockdown followed by treatment with or without insulin. A total of 16 samples from 4 sets of experiments were analyzed: cells treated without Dox & without insulin (NoDox_Bas, n=4), cells treated without Dox & with insulin (NoDox_Ins, n=4), cells treated with Dox & without insulin (Dox_Bas, n=4), and cells treated with Dox & with insulin (Dox_Ins, n=4). The experimental flow-chart is shown in Fig. 2. In total, 3876 phosphorylation sites were identified. Among them, 3192 are phosphoserines (82.4%), 410 are phosphothreonines (10.6%), and 274 are phosphotyrosines (7.1%), giving a pS/pT/pY ratio at 23:3:2. This ratio was similar to that reported previously in human skeletal muscle by our group (the pS/pT/pY ratio was ~18:4:1) [27]. Of the 3876 phosphosites, 908 sites have not been reported in rat according to the largest phosphorylation site databases, http://www.phosphosite.org and the largest phosphoproteome data set derived from rat tissues containing 31480 phosphorylation sites [33]. Among the 908 sites, 620 sites have not been reported in any species, thus appear to be novel (Supplemental Table 1).

There were 3731 non-labeled phosphorylation sites assigned to 1234 proteins from the sixteen samples, and these phosphorylation sites were derived from the L6K76 cells. Ingenuity Pathway Analysis (IPA) on these 1234 proteins revealed 21 significantly enriched pathways with $P < 0.01$ related to skeletal muscle cell function and signaling. Among them, multiple pathways are related to insulin signaling, such as insulin receptor signaling, mTOR

signaling, RhoA Signaling, and ERK/MAPK signaling (Supplemental Table 2, Supplemental Fig. 1). In addition, there were multiple pathways related to cellular junctions, such as focal adhesion kinase (FAK) signaling, integrin signaling, tight junction signaling and integrin-linked kinase (ILK) signaling.

3.3 Phosphorylation changes in response to PPP1R12A knockdown

The overall phosphorylation levels were evaluated using isotope-labeled phosphosites identified in all the sixteen samples as a "Universal Standard". The total peak area of these isotope-labeled phosphosites (I_u) was obtained and used to normalize the total peak area of all non-labeled phosphosites (I_L). As shown in Table 1, PPP1R12A knockdown significantly increased overall phosphorylation level in the cells at basal state ($P < 0.01$). This effect was not observed after insulin stimulation. In addition, insulin stimulation in cells with or without PPP1R12A knockdown did not result in overall phosphorylation changes.

In total, 698 phosphorylation sites were affected by PPP1R12A knockdown at basal and insulin stimulation states (Supplemental table 3). Under the basal condition (Bas_NoDox *vs*. Bas_Dox), 544 sites significantly changed after PPP1R12A knockdown, and among them, 470 phosphorylation sites showed increased phosphorylation, and 74 sites had decreased phosphorylation. After insulin stimulation, PPP1R12A knockdown resulted in 115 phosphorylation sites with increased phosphorylation and 95 phosphosites with decreased phosphorylation. It is noted that the phosphorylation levels of 56 phosphorylation sites were changed significantly at both basal and insulin-stimulated conditions after PPP1R12A knockdown. Among them, 21 sites had increased phosphorylation at both states; 3 sites had decreased phosphorylation at both states; and 32 phosphosites had opposite trends (Supplemental Table 3).

These 698 phosphosites were assigned to 295 proteins including multiple protein kinases, such as serine/threonine-protein kinase D 3 (PKD3), AP2-associated protein kinase 1(AAK1), proto-oncogene tyrosine-protein kinase Src (c-Src), STE20-like serine/threonine-protein kinase (SLK), mitogen-activated protein kinase kinase kinase 7 (TAK1), serine/threonine-protein kinase TAO3, serine/threonine-protein kinase PRP4 homolog and serine/threonine-protein kinase DCLK1. The assigned phosphatases include sphingosine-1-phosphate phosphatase 1 (hSPP1) and carboxyl-terminal domain phosphatase, subunit 1(FCP1).

Multiple reported PPP1R12A interaction partners in reference [11] are among the 295 proteins with phosphorylation sites affected by PPP1R12A knockdown, such as α-adducin (gene name: Add1); Heat shock 27 kDa protein 1 (gene name: Hspb1), and Myosin phosphatase Rho-interacting protein (also known as M-RIP, gene name: Mprip). All of them had significantly increased site-specific phosphorylation after PPP1R12A knockdown under the basal condition ($P < 0.05$, Table 2). In addition, as discussed before, we have recently identified PPP1R12A as a novel endogenous interaction partner with insulin receptor substrate 1 (IRS1) [19]. In the present study, PPP1R12A knockdown led to a significantly increased phosphorylation level of pS522 of IRS1 under the insulin stimulated condition ($P < 0.05$, Table 2).

3.4 PPP1R12A knockdown affected signaling pathways

For the 295 proteins containing phosphosites affected by PPP1R12A knockdown, Ingenuity Pathway Analysis (IPA) was used to analyze signal pathway networks and canonical pathways. The network with the highest score is “RNA Post-Transcriptional Modification, Gene Expression, Molecular Transport”, which contains total 35 proteins, and among them, 31 proteins had phosphorylation sites affected by PPP1R12A knockdown in this study (Fig. 3).

From the 295 phosphoproteins (Supplemental Table 3) affected by PPP1R12A knockdown, IPA revealed proteins involved in pathways related to insulin signaling, such as insulin receptor signaling, mTOR signaling, RhoA signaling and ERK/MAPK signaling, etc (Supplemental Table 2, highlighted in bold). In addition, proteins involved in cellular junctions also were significantly enriched. The phosphorylation changes of proteins related to insulin signaling were summarized in Table 2.

4. Discussion

Insulin is a potent anabolic hormone that modulates a wide variety of biological processes in skeletal muscle, including glycogen synthesis, glucose transport, mitogenesis, and protein synthesis. Insulin induced protein phosphorylation and dephosphorylation is a key to linking events at the plasma membrane with intracellular machinery. Abnormalities in this process are considered to be one of the main contributing factors to for a large number of disease conditions, such as insulin resistance, the metabolic syndrome, and T2D. Extensive research has been carried out to study the role of kinases in insulin action. However, a mechanism for serine/threonine phosphatase action in insulin signal transduction is largely unknown. Recent evidences from our group suggest that PPP1R12A, a regulatory subunit of protein phosphatase 1, is involved in insulin signaling [19–21]. Moreover, the majority of research on the abnormalities of phosphorylation in skeletal muscle insulin action focuses a few known phosphorylation targets. Therefore, we optioned to use quantitative phosphoproteomics to generate a global picture of phosphorylation events regulated by PPP1R12A in L6 cells, which have been engineered for inducible PPP1R12Aknockdown. We found that PPP1R12A knockdown affected numerous pathways related to insulin signaling in L6 cells, suggesting that PP1 have multiple targets in insulin action through its subunit PPP1R12A.

4.1 PPP1R12A regulates global protein phosphorylation in L6 cells

PP1 regulates a large variety of cellular processes through serine and threonine dephosphorylation events in eukaryotes [8–10]. The specificity and activity of PP1 catalytic subunit can be tuned by its regulatory subunits including PPP1R12A [8–10]. Therefore, we hypothesized that knockdown PPP1R12A will lead to decreased specificity and activity of PP1c, and subsequent phosphorylation increase for the proteins regulated by the PP1c/PPP1R12A complex. To test our hypothesis, we developed a L6 cell line (designated L6K76) which allows more than 80% knockdown of PPP1R12A at induction of doxycycline. We found that PPP1R12A knockdown led to overall phosphorylation increase in L6 cells (Table 1) and the increased phosphorylation for 470 sites (compared to only

decreased phosphorylation for 74 sites) at the basal condition (Supplemental Table 3). This hypothesis was supported by these findings. Of note, the PPP1R12A S507 phosphorylation was reduced to 21% as a result of reduced total PPP1R12A protein (Fig. 1, Table 2, Supplemental 3).

There were 698 phosphorylation sites with a significant change at basal or insulin stimulated states in response to PPP1R12A knockdown. Among them, 695 were serine/threonine sites and only 3 are phosphotyrosine sites, which is expected since one main function of PPP1R12A is to increase the activity & specificity of the catalytic subunit of serine/threonine protein phosphatase 1 (PP1c) against its substrates [11, 14, 15]. These results provided the first evidence that PPP1R12A indeed regulates a large number of serine/threonine phosphorylation events in L6 cells. Please note that the PP1c/PPP1R12A complex may regulate these phosphorylation sites directly or indirectly via other proteins, such as kinases.

4.2 PPP1R12A affected multiple pathways related to insulin signaling

As discussed before, little is known about the phosphorylation events controlled by the PPP1R12A in the context of skeletal muscle insulin signaling. PPP1R12A knockdown offers an opportunity to discover potential new substrates of PP1 in insulin signaling pathways. We identified serine/threonine sites whose phosphorylation states were changed significantly at basal and/or insulin-stimulated conditions due to knockdown of PPP1R12A, a PP1 regulatory subunit. The corresponding phosphoproteins are assigned to multiple significantly enriched pathways related to insulin signaling (Supplemental Table 2), such as mTOR signaling and RhoA signaling.

4.3 mTOR signaling

The mTOR signaling pathway serves as a central regulator of cell metabolism, growth, proliferation and survival. There are two major mTOR complexes, mTOR complex 1 (mTORC1) and mTOR complex 2 (mTORC2) [40, 41]. mTORC1 comprises the catalytic subunit mTOR, the regulatory protein raptor (Raptor), proline rich Akt substrate 40 kDa (PRAS40, also known as Akt1s1), DEP-domain-containing mTOR-interacting protein (Deptor) and GbL [42]. Raptor plays an important role as a scaffolding protein to recruit substrates p70S6K and eukaryotic initiation factor 4E-binding protein 1 (4E-BP1), two key regulators of mRNA translation and ribosome biogenesis [43–47]. In response to insulin stimulation and nutrient sufficiency, raptor can positively regulate mTOR activity by enhancing its binding to substrates [48–51], and by interacting with Rag family GTPases to induce mTOR complex relocalization [52–54]. Phosphorylation of raptor S863 by either mTOR or ERK1/2 promotes mTORC1 activation in response to various stimuli, including growth factors, nutrients, and cellular energy [55–58]. The raptor S859 is also phosphorylated in response to insulin stimulation, but in a S863-dependent manner [55]. In this study PPP1R12A knockdown resulted in 2.8-fold and 5.6-fold increased basal phosphorylation of raptor S863 and S859 ($P < 0.01$ for both sites, Table 2), suggesting that the PP1c/PPP1R12A complex might regulate mTORC1 through raptor S863 and S859.

PRAS40/Akt1s1 and Deptor are negative regulators of mTORC1 [42, 49, 59]. PRAS40 may regulate mTORC1 kinase activity by functioning as a direct inhibitor of substrate binding [60]. Insulin stimulates Akt/PKB-mediated phosphorylation of human PRAS40 on T246 (rat T247), which prevents its inhibition of mTORC1 [49, 61–63]. The PRAS40 S88 is an insulin stimulated phosphosite [64], but its function in mTORC1 regulation is unknown. We found that PRAS40 T247 phosphorylation level reduced to 32.9% ($P < 0.05$), while PRAS40 S88 phosphorylation increased 1.7 fold in response to PPP1R12A knockdown at the basal state.

mTORC2 can phosphorylate multiple kinases such as Akt, SGK (serum- and glucocorticoid-induced protein kinase) and PKC, which play an important role in cell survival, cell cycle progression and anabolism [65–68]. PKD3 belongs to the PKC family (also classified to PKD family recently [69]), which is responsive to diacylglycerol (DAG), growth factors and phorbol 12-myristate 13-acetate (PMA). Unlike other PKC members, the link between mTORC2 and PKD3 is still missing. PKD3 regulates paxillin trafficking and cellular protrusive activity [70]. As a result of PPP1R12A knockdown, PKD3 S213/S216 phosphorylation increased 3.5 folds ($P < 0.05$). It is interesting to determine whether the phosphorylation change is related to any cytoskeleton rearrangement that is critical to insulin signaling.

An important biological function of insulin is to stimulate protein synthesis in skeletal muscle. Reduced mitochondrial protein synthesis has been observed in type 2 diabetic patients compared to matched control subjects [71]. Initiation is generally the rate limiting phase in translation [72]. PPP1R12A knockdown affected the phosphorylation state of four translation initiation regulators in mTOR signaling pathway, eIF-3G, eIF-3B, eIF-4B and RPS6. We observed decreased phosphorylation with eIF-3G (T41), and increased phosphorylation with eIF-3B (S75, S79) and eIF-4B (S425). However, further study is needed to investigate the functions of these phosphorylation sites. In addition, phosphorylation of RPS6, a component protein of the small 40 S ribosomal subunit [73], plays a critical role in mRNA translation initiation and protein synthesis [74–79]. Insulin-induced increase in RPS6 phosphorylation is mediated by the mTOR/FRAP-p70S6K pathway [73, 80] and the RAS/ERK/p90 ribosomal S6K kinase pathway [75, 81]. Mice deficient in ribosomal protein S6 phosphorylation suffer from muscle weakness that reflects a growth defect and energy deficit [82]. Furthermore, depletion or overexpression dominant-negative PP1c increased RPS6 C terminus phosphorylation [76], suggesting that these phosphorylation sites were regulated by PP1. In the current work, we also observed the increased phosphorylation of RPS6 on multiple sites (S235, S236, S240, S244 and S247) at basal and insulin-stimulated states (Table 2). We performed WB analyses to confirm the effect of PPP1R12A knock-down on RPS6 phosphorylation. As can be seen from Fig. 4, PPP1R12A knockdown led to increased S240/244 phosphorylation at both basal and insulin-stimulated states, which is consistent with the results obtained by HPLC-ESI-MS/MS (Table 2). These results implied that these phosphorylation sites in RPS6 were regulated by PPP1R12A, most likely through PP1c.

4.4 RhoA signaling pathways

RhoA is a member of the Ras superfamily of small GTPases that plays a central role in diverse biological processes such as cytoskeletal reorganization, membrane trafficking, cytokinesis, and stress fiber contraction. Insulin negatively modulates RhoA signaling and impacts actin cytoskeleton organization [83]. After PPP1R12A knockdown, increased phosphorylation was observed for six proteins in RhoA signaling, including RhoGAP5 (S1173 and S1176), MRIP (S294), cofilin-1 (S3), ARHGEF11 (S671/ T676), septin-9 (S12, T24) and BORG4 (S136/S140), implying they are potential substrates of the PP1c/ PPP1R12A phosphatase. Cofilin-1 is one of the actin-binding proteins. Cofilin-1 activity is inhibited by the phosphorylation of the serine residue at position 3 (S3) [84, 85]. LIM-kinases (LIMKs) and related testicular protein kinases (TESKs) specifically phosphorylate cofilin-1 at S3 and thereby inhibit the actin binding, severing, and depolymerizing activities of cofilin [86–90]. Slingshot family protein phosphatases (SSHs) specifically dephosphorylate and reactivate S3-phosphorylated cofilin (P-cofilin) [91, 92]. Serine/ threonine protein phosphatase 1 (PP1) [93], protein phosphatase 2A (PP2A) [93], chronophin (CIN, a haloacid dehalogenase) [94, 95] have also been shown to be involved in cofilin dephosphorylation. The MRIP has been found as an insulin-stimulated PPP1R12A interaction partner [96], and whether S294 of MRIP plays a role in this interaction is currently unknown. The septin-9 and BORG4 are cytoskeletal proteins regulating cytokenesis. Human septin-9 isoform c (NP_006631.2) T24 (equivalent to rat septin-9 T24) is phosphorylated by cyclin-dependent kinase 1 (Cdk1) to create a binding site for the WW domain of Pin1, which, in turn, induces a conformational change in the N-terminal of septin-9 [97]. The Pin1-septin-9 interaction is important for the completion of cytokinesis [97]. Our results imply that the PP1c/PPP1R12A phosphatase might be involved in cytokinesis through dephosphorylating septin-9 T24 and BORG4 S136/S140.

5. Conclusions

In summary, we created the first doxycycline (Dox) inducible PPP1R12A knockdown L6 cell line and identified over 600 novel phosphosites in L6 cells using phosphoproteomics. Furthermore, we provided the first global view of phosphorylation changes caused by PPP1R12A knockdown, and discovered numerous phosphorylation sites in multiple pathways regulated by PPP1R12A in the context of insulin action. These results indicate that PPP1R12A indeed plays a role in skeletal muscle insulin signaling, providing novel insights into the biology of insulin signaling. This information will facilitate the design of experiments to better understand the molecular mechanism responsible for skeletal muscle insulin resistance and associated diseases, such as type 2 diabetes and cardiovascular diseases.

Supplementary Material

Refer to Web version on PubMed Central for supplementary material.

Acknowledgments

This work was supported by NIH/NIDDK R01DK081750 (ZY), R01DK081750-04S1 (ML/ZY), Wayne State University faculty competition for post-doctoral fellow award (MC/ZY), and Wayne State University faculty start-up (ZY).

References

1. Rask-Madsen C, Kahn CR. Tissue-specific insulin signaling, metabolic syndrome, and cardiovascular disease. Arterioscler Thromb Vasc Biol. 2012; 32:2052–9. [PubMed: 22895666]
2. Saini V. Molecular mechanisms of insulin resistance in type 2 diabetes mellitus. World J Diabetes. 2011; 1:68–75. [PubMed: 21537430]
3. Abdul-Ghani MA, DeFronzo RA. Pathogenesis of insulin resistance in skeletal muscle. J Biomed Biotechnol. 2010; 2010:476279. [PubMed: 20445742]
4. Biddinger SB, Kahn CR. From mice to men: insights into the insulin resistance syndromes. Annu Rev Physiol. 2006; 68:123–58. [PubMed: 16460269]
5. Hojlund K, Beck-Nielsen H. Impaired glycogen synthase activity and mitochondrial dysfunction in skeletal muscle. Markers or mediators in type 2 diabetes. Current Diabetes Reviews. 2006; 2:375–95. [PubMed: 18220643]
6. Lowell BB, Shulman GI. Mitochondrial dysfunction and type 2 diabetes. Science. 2005; 307:384–7. [PubMed: 15662004]
7. Pirola L, Johnston AM, Van Obberghen E. Modulation of insulin action. Diabetologia. 2004; 47:170–84. [PubMed: 14722654]
8. Bollen M, Peti W, Ragusa MJ, Beullens M. The extended PP1 toolkit: designed to create specificity. Trends Biochem Sci. 2010; 35:450–8. [PubMed: 20399103]
9. Cohen PT. Protein phosphatase 1--targeted in many directions. J Cell Sci. 2002; 115:241–56. [PubMed: 11839776]
10. Virshup DM, Shenolikar S. From promiscuity to precision: protein phosphatases get a makeover. Mol Cell. 2009; 33:537–45. [PubMed: 19285938]
11. Matsumura F, Hartshorne DJ. Myosin phosphatase target subunit: Many roles in cell function. Biochem Biophys Res Commun. 2008; 369:149–56. [PubMed: 18155661]
12. Okamoto R, Ito M, Suzuki N, Kongo M, Moriki N, Saito H, et al. The targeted disruption of the MYPT1 gene results in embryonic lethality. Transgenic Res. 2005; 14:337–40. [PubMed: 16145842]
13. He WQ, Qiao YN, Peng YJ, Zha JM, Zhang CH, Chen C, et al. Altered contractile phenotypes of intestinal smooth muscle in mice deficient in myosin phosphatase target subunit 1. Gastroenterology. 2013; 144:1456–65. 65 e1–5. [PubMed: 23499953]
14. Okamoto R, Kato T, Mizoguchi A, Takahashi N, Nakakuki T, Mizutani H, et al. Characterization and function of MYPT2, a target subunit of myosin phosphatase in heart. Cell Signal. 2006; 18:1408–16. [PubMed: 16431080]
15. Grassie ME, Moffat LD, Walsh MP, Macdonald JA. The myosin phosphatase targeting protein (MYPT) family: a regulated mechanism for achieving substrate specificity of the catalytic subunit of protein phosphatase type 1δ. Arch Biochem Biophys. 2011; 510:147–59. [PubMed: 21291858]
16. Ito M, Nakano T, Erdodi F, Hartshorne DJ. Myosin phosphatase: structure, regulation and function. Mol Cell Biochem. 2004; 259:197–209. [PubMed: 15124925]
17. Moorhead G, Johnson D, Morrice N, Cohen P. The major myosin phosphatase in skeletal muscle is a complex between the β-isoform of protein phosphatase 1 and the MYPT2 gene product. FEBS letters. 1998; 438:141–4. [PubMed: 9827534]
18. Yamashiro S, Yamakita Y, Totsukawa G, Goto H, Kaibuchi K, Ito M, et al. Myosin phosphatase-targeting subunit 1 regulates mitosis by antagonizing polo-like kinase 1. Dev Cell. 2008; 14:787–97. [PubMed: 18477460]
19. Geetha T, Langlais P, Luo M, Mapes R, Lefort N, Chen SC, et al. Label-free proteomic identification of endogenous, insulin-stimulated interaction partners of insulin receptor substrate-1. Journal of the American Society for Mass Spectrometry. 2011; 22:457–66. [PubMed: 21472564]

20. Geetha T, Langlais P, Caruso M, Yi Z. Protein phosphatase 1 regulatory subunit 12A and catalytic subunit δ, new members in the phosphatidylinositide 3 kinase insulin-signaling pathway. The Journal of endocrinology. 2012; 214:437–43. [PubMed: 22728334]
21. Chao A, Zhang X, Ma D, Langlais P, Luo M, Mandarino LJ, et al. Site-specific phosphorylation of protein phosphatase 1 regulatory subunit 12A stimulated or suppressed by insulin. Journal of proteomics. 2012; 75:3342–50. [PubMed: 22516431]
22. Wiederschain D, Wee S, Chen L, Loo A, Yang G, Huang A, et al. Single-vector inducible lentiviral RNAi system for oncology target validation. Cell Cycle. 2009; 8:498–504. [PubMed: 19177017]
23. Kutner RH, Zhang XY, Reiser J. Production, concentration and titration of pseudotyped HIV-1-based lentiviral vectors. Nature protocols. 2009; 4:495–505.
24. Gruhler A, Olsen JV, Mohammed S, Mortensen P, Faergeman NJ, Mann M, et al. Quantitative phosphoproteomics applied to the yeast pheromone signaling pathway. Molecular & cellular proteomics : MCP. 2005; 4:310–27. [PubMed: 15665377]
25. Ma DJ, Li SJ, Wang LS, Dai J, Zhao SL, Zeng R. Temporal and spatial profiling of nuclei-associated proteins upon TNF-α/NF-κB signaling. Cell research. 2009; 19:651–64. [PubMed: 19399029]
26. Ong SE, Blagoev B, Kratchmarova I, Kristensen DB, Steen H, Pandey A, et al. Stable isotope labeling by amino acids in cell culture, SILAC, as a simple and accurate approach to expression proteomics. Molecular & cellular proteomics : MCP. 2002; 1:376–86. [PubMed: 12118079]
27. Hojlund K, Bowen BP, Hwang H, Flynn CR, Madireddy L, Geetha T, et al. In vivo phosphoproteome of human skeletal muscle revealed by phosphopeptide enrichment and HPLC-ESI-MS/MS. Journal of proteome research. 2009; 8:4954–65. [PubMed: 19764811]
28. Cox J, Mann M. MaxQuant enables high peptide identification rates, individualized p.p.b.-range mass accuracies and proteome-wide protein quantification. Nature biotechnology. 2008; 26:1367–72.
29. Cox J, Matic I, Hilger M, Nagaraj N, Selbach M, Olsen JV, et al. A practical guide to the MaxQuant computational platform for SILAC-based quantitative proteomics. Nature protocols. 2009; 4:698–705.
30. Neuhauser N, Michalski A, Cox J, Mann M. Expert system for computer-assisted annotation of MS/MS spectra. Molecular & cellular proteomics : MCP. 2012; 11:1500–9. [PubMed: 22888147]
31. de Godoy LM, Olsen JV, Cox J, Nielsen ML, Hubner NC, Frohlich F, et al. Comprehensive mass-spectrometry-based proteome quantification of haploid versus diploid yeast. Nature. 2008; 455:1251–4. [PubMed: 18820680]
32. Monetti M, Nagaraj N, Sharma K, Mann M. Large-scale phosphosite quantification in tissues by a spike-in SILAC method. Nat Methods. 8:655–8. [PubMed: 21743459]
33. Lundby A, Secher A, Lage K, Nordsborg NB, Dmytriyev A, Lundby C, et al. Quantitative maps of protein phosphorylation sites across 14 different rat organs and tissues. Nat Commun. 2012; 3:876. [PubMed: 22673903]
34. Olsen JV, Blagoev B, Gnad F, Macek B, Kumar C, Mortensen P, et al. Global, in vivo, and site-specific phosphorylation dynamics in signaling networks. Cell. 2006; 127:635–48. [PubMed: 17081983]
35. Martinez E, Gerard N, Garcia MM, Mazur A, Gueant-Rodriguez RM, Comte B, et al. Myocardium proteome remodelling after nutritional deprivation of methyl donors. The Journal of nutritional biochemistry. 2013; 24:1241–50. [PubMed: 23318136]
36. Ye Y, Yan G, Luo Y, Tong T, Liu X, Xin C, et al. Quantitative proteomics by amino acid labeling in foot-and-mouth disease virus (FMDV)-infected cells. Journal of proteome research. 2013; 12:363–77. [PubMed: 23170859]
37. Thomas S, Bonchev D. A survey of current software for network analysis in molecular biology. Human genomics. 2010; 4:353–60. [PubMed: 20650822]
38. Jimenez-Marin A, Collado-Romero M, Ramirez-Boo M, Arce C, Garrido JJ. Biological pathway analysis by ArrayUnlock and Ingenuity Pathway Analysis. BMC Proc. 2009; 3 (Suppl 4):S6. [PubMed: 19615119]

39. Werner T. Bioinformatics applications for pathway analysis of microarray data. Curr Opin Biotechnol. 2008; 19:50–4. [PubMed: 18207385]
40. Guertin DA, Sabatini DM. Defining the role of mTOR in cancer. Cancer cell. 2007; 12:9–22. [PubMed: 17613433]
41. Loewith R, Jacinto E, Wullschleger S, Lorberg A, Crespo JL, Bonenfant D, et al. Two TOR complexes, only one of which is rapamycin sensitive, have distinct roles in cell growth control. Mol Cell. 2002; 10:457–68. [PubMed: 12408816]
42. Peterson TR, Laplante M, Thoreen CC, Sancak Y, Kang SA, Kuehl WM, et al. DEPTOR is an mTOR inhibitor frequently overexpressed in multiple myeloma cells and required for their survival. Cell. 2009; 137:873–86. [PubMed: 19446321]
43. Ma XM, Blenis J. Molecular mechanisms of mTOR-mediated translational control. Nature reviews Molecular cell biology. 2009; 10:307–18.
44. Fingar DC, Richardson CJ, Tee AR, Cheatham L, Tsou C, Blenis J. mTOR controls cell cycle progression through its cell growth effectors S6K1 and 4E-BP1/eukaryotic translation initiation factor 4E. Molecular and cellular biology. 2004; 24:200–16. [PubMed: 14673156]
45. Hara K, Yonezawa K, Kozlowski MT, Sugimoto T, Andrabi K, Weng QP, et al. Regulation of eIF-4E BP1 phosphorylation by mTOR. The Journal of biological chemistry. 1997; 272:26457–63. [PubMed: 9334222]
46. Proud CG. mTOR-mediated regulation of translation factors by amino acids. Biochem Biophys Res Commun. 2004; 313:429–36. [PubMed: 14684180]
47. Nojima H, Tokunaga C, Eguchi S, Oshiro N, Hidayat S, Yoshino K, et al. The mammalian target of rapamycin (mTOR) partner, raptor, binds the mTOR substrates p70 S6 kinase and 4E-BP1 through their TOR signaling (TOS) motif. The Journal of biological chemistry. 2003; 278:15461–4. [PubMed: 12604610]
48. Wang L, Harris TE, Lawrence JC Jr. Regulation of proline-rich Akt substrate of 40 kDa (PRAS40) function by mammalian target of rapamycin complex 1 (mTORC1)-mediated phosphorylation. The Journal of biological chemistry. 2008; 283:15619–27. [PubMed: 18372248]
49. Sancak Y, Thoreen CC, Peterson TR, Lindquist RA, Kang SA, Spooner E, et al. PRAS40 is an insulin-regulated inhibitor of the mTORC1 protein kinase. Mol Cell. 2007; 25:903–15. [PubMed: 17386266]
50. Nascimento EB, Ouwens DM. PRAS40: target or modulator of mTORC1 signalling and insulin action? Archives of physiology and biochemistry. 2009; 115:163–75. [PubMed: 19480563]
51. Fonseca BD, Smith EM, Lee VH, MacKintosh C, Proud CG. PRAS40 is a target for mammalian target of rapamycin complex 1 and is required for signaling downstream of this complex. The Journal of biological chemistry. 2007; 282:24514–24. [PubMed: 17604271]
52. Kim E, Goraksha-Hicks P, Li L, Neufeld TP, Guan KL. Regulation of TORC1 by Rag GTPases in nutrient response. Nature cell biology. 2008; 10:935–45.
53. Sancak Y, Peterson TR, Shaul YD, Lindquist RA, Thoreen CC, Bar-Peled L, et al. The Rag GTPases bind raptor and mediate amino acid signaling to mTORC1. Science. 2008; 320:1496–501. [PubMed: 18497260]
54. Hanrahan J, Blenis J. Rheb activation of mTOR and S6K1 signaling. Methods in enzymology. 2006; 407:542–55. [PubMed: 16757352]
55. Foster KG, Acosta-Jaquez HA, Romeo Y, Ekim B, Soliman GA, Carriere A, et al. Regulation of mTOR complex 1 (mTORC1) by raptor Ser863 and multisite phosphorylation. The Journal of biological chemistry. 2010; 285:80–94. [PubMed: 19864431]
56. Carriere A, Romeo Y, Acosta-Jaquez HA, Moreau J, Bonneil E, Thibault P, et al. ERK1/2 phosphorylate Raptor to promote Ras-dependent activation of mTOR complex 1 (mTORC1). The Journal of biological chemistry. 2011; 286:567–77. [PubMed: 21071439]
57. Wang L, Lawrence JC Jr, Sturgill TW, Harris TE. Mammalian target of rapamycin complex 1 (mTORC1) activity is associated with phosphorylation of raptor by mTOR. The Journal of biological chemistry. 2009; 284:14693–7. [PubMed: 19346248]
58. Frey JW, Jacobs BL, Goodman CA, Hornberger TA. A role for Raptor phosphorylation in the mechanical activation of mTOR signaling. Cell Signal. 2014; 26:313–22. [PubMed: 24239769]

59. Vander Haar E, Lee SI, Bandhakavi S, Griffin TJ, Kim DH. Insulin signalling to mTOR mediated by the Akt/PKB substrate PRAS40. Nature cell biology. 2007; 9:316–23.
60. Wang L, Harris TE, Roth RA, Lawrence JC Jr. PRAS40 regulates mTORC1 kinase activity by functioning as a direct inhibitor of substrate binding. The Journal of biological chemistry. 2007; 282:20036–44. [PubMed: 17510057]
61. Kovacina KS, Park GY, Bae SS, Guzzetta AW, Schaefer E, Birnbaum MJ, et al. Identification of a proline-rich Akt substrate as a 14-3-3 binding partner. The Journal of biological chemistry. 2003; 278:10189–94. [PubMed: 12524439]
62. Volkers M, Toko H, Doroudgar S, Din S, Quijada P, Joyo AY, et al. Pathological hypertrophy amelioration by PRAS40-mediated inhibition of mTORC1. Proceedings of the National Academy of Sciences of the United States of America. 2013; 110:12661–6. [PubMed: 23842089]
63. Nascimento EB, Snel M, Guigas B, van der Zon GC, Kriek J, Maassen JA, et al. Phosphorylation of PRAS40 on Thr246 by PKB/AKT facilitates efficient phosphorylation of Ser183 by mTORC1. Cell Signal. 2010; 22:961–7. [PubMed: 20138985]
64. Yu Y, Yoon SO, Poulogiannis G, Yang Q, Ma XM, Villen J, et al. Phosphoproteomic analysis identifies Grb10 as an mTORC1 substrate that negatively regulates insulin signaling. Science. 2011; 332:1322–6. [PubMed: 21659605]
65. Facchinetti V, Ouyang W, Wei H, Soto N, Lazorchak A, Gould C, et al. The mammalian target of rapamycin complex 2 controls folding and stability of Akt and protein kinase C. The EMBO journal. 2008; 27:1932–43. [PubMed: 18566586]
66. Garcia-Martinez JM, Alessi DR. mTOR complex 2 (mTORC2) controls hydrophobic motif phosphorylation and activation of serum- and glucocorticoid-induced protein kinase 1 (SGK1). The Biochemical journal. 2008; 416:375–85. [PubMed: 18925875]
67. Ikenoue T, Inoki K, Yang Q, Zhou X, Guan KL. Essential function of TORC2 in PKC and Akt turn motif phosphorylation, maturation and signalling. The EMBO journal. 2008; 27:1919–31. [PubMed: 18566587]
68. Sarbassov DD, Guertin DA, Ali SM, Sabatini DM. Phosphorylation and regulation of Akt/PKB by the rictor-mTOR complex. Science. 2005; 307:1098–101. [PubMed: 15718470]
69. Manning G, Whyte DB, Martinez R, Hunter T, Sudarsanam S. The protein kinase complement of the human genome. Science. 2002; 298:1912–34. [PubMed: 12471243]
70. Huck B, Kemkemer R, Franz-Wachtel M, Macek B, Hausser A, Olayioye MA. GIT1 phosphorylation on serine 46 by PKD3 regulates paxillin trafficking and cellular protrusive activity. The Journal of biological chemistry. 2012; 287:34604–13. [PubMed: 22893698]
71. Halvatsiotis P, Short KR, Bigelow M, Nair KS. Synthesis rate of muscle proteins, muscle functions, and amino acid kinetics in type 2 diabetes. Diabetes. 2002; 51:2395–404. [PubMed: 12145150]
72. Gingras AC, Raught B, Sonenberg N. eIF4 initiation factors: effectors of mRNA recruitment to ribosomes and regulators of translation. Annual review of biochemistry. 1999; 68:913–63.
73. Meyuhas O. Physiological roles of ribosomal protein S6: one of its kind. International review of cell and molecular biology. 2008; 268:1–37. [PubMed: 18703402]
74. Krieg J, Hofsteenge J, Thomas G. Identification of the 40 S ribosomal protein S6 phosphorylation sites induced by cycloheximide. The Journal of biological chemistry. 1988; 263:11473–7. [PubMed: 3403539]
75. Roux PP, Shahbazian D, Vu H, Holz MK, Cohen MS, Taunton J, et al. RAS/ERK signaling promotes site-specific ribosomal protein S6 phosphorylation via RSK and stimulates cap-dependent translation. The Journal of biological chemistry. 2007; 282:14056–64. [PubMed: 17360704]
76. Hutchinson JA, Shanware NP, Chang H, Tibbetts RS. Regulation of ribosomal protein S6 phosphorylation by casein kinase 1 and protein phosphatase 1. The Journal of biological chemistry. 2011; 286:8688–96. [PubMed: 21233202]
77. Martin-Perez J, Thomas G. Ordered phosphorylation of 40S ribosomal protein S6 after serum stimulation of quiescent 3T3 cells. Proceedings of the National Academy of Sciences of the United States of America. 1983; 80:926–30. [PubMed: 6573662]

78. Wettenhall RE, Erikson E, Maller JL. Ordered multisite phosphorylation of Xenopus ribosomal protein S6 by S6 kinase II. The Journal of biological chemistry. 1992; 267:9021–7. [PubMed: 1577739]

79. Miranda L, Horman S, De Potter I, Hue L, Jensen J, Rider MH. Effects of contraction and insulin on protein synthesis, AMP-activated protein kinase and phosphorylation state of translation factors in rat skeletal muscle. Pflugers Archiv : European journal of physiology. 2008; 455:1129–40. [PubMed: 17957382]

80. von Manteuffel SR, Dennis PB, Pullen N, Gingras AC, Sonenberg N, Thomas G. The insulin-induced signalling pathway leading to S6 and initiation factor 4E binding protein 1 phosphorylation bifurcates at a rapamycin-sensitive point immediately upstream of p70s6k. Molecular and cellular biology. 1997; 17:5426–36. [PubMed: 9271419]

81. Pende M, Um SH, Mieulet V, Sticker M, Goss VL, Mestan J, et al. S6K1(−/−)/S6K2(−/−) mice exhibit perinatal lethality and rapamycin-sensitive 5′-terminal oligopyrimidine mRNA translation and reveal a mitogen-activated protein kinase-dependent S6 kinase pathway. Molecular and cellular biology. 2004; 24:3112–24. [PubMed: 15060135]

82. Ruvinsky I, Katz M, Dreazen A, Gielchinsky Y, Saada A, Freedman N, et al. Mice deficient in ribosomal protein S6 phosphorylation suffer from muscle weakness that reflects a growth defect and energy deficit. PloS one. 2009; 4:e5618. [PubMed: 19479038]

83. Begum N, Sandu OA, Duddy N. Negative regulation of rho signaling by insulin and its impact on actin cytoskeleton organization in vascular smooth muscle cells: role of nitric oxide and cyclic guanosine monophosphate signaling pathways. Diabetes. 2002; 51:2256–63. [PubMed: 12086958]

84. Agnew BJ, Minamide LS, Bamburg JR. Reactivation of phosphorylated actin depolymerizing factor and identification of the regulatory site. The Journal of biological chemistry. 1995; 270:17582–7. [PubMed: 7615564]

85. Moriyama K, Iida K, Yahara I. Phosphorylation of Ser-3 of cofilin regulates its essential function on actin. Genes to cells : devoted to molecular & cellular mechanisms. 1996; 1:73–86. [PubMed: 9078368]

86. Petrilli A, Copik A, Posadas M, Chang LS, Welling DB, Giovannini M, et al. LIM domain kinases as potential therapeutic targets for neurofibromatosis type 2. Oncogene. 2013

87. Yang N, Higuchi O, Ohashi K, Nagata K, Wada A, Kangawa K, et al. Cofilin phosphorylation by LIM-kinase 1 and its role in Rac-mediated actin reorganization. Nature. 1998; 393:809–12. [PubMed: 9655398]

88. Arber S, Barbayannis FA, Hanser H, Schneider C, Stanyon CA, Bernard O, et al. Regulation of actin dynamics through phosphorylation of cofilin by LIM-kinase. Nature. 1998; 393:805–9. [PubMed: 9655397]

89. Sumi T, Matsumoto K, Takai Y, Nakamura T. Cofilin phosphorylation and actin cytoskeletal dynamics regulated by rho- and Cdc42-activated LIM-kinase 2. The Journal of cell biology. 1999; 147:1519–32. [PubMed: 10613909]

90. Toshima J, Toshima JY, Amano T, Yang N, Narumiya S, Mizuno K. Cofilin phosphorylation by protein kinase testicular protein kinase 1 and its role in integrin-mediated actin reorganization and focal adhesion formation. Molecular biology of the cell. 2001; 12:1131–45. [PubMed: 11294912]

91. Niwa R, Nagata-Ohashi K, Takeichi M, Mizuno K, Uemura T. Control of actin reorganization by Slingshot, a family of phosphatases that dephosphorylate ADF/cofilin. Cell. 2002; 108:233–46. [PubMed: 11832213]

92. Ohta Y, Kousaka K, Nagata-Ohashi K, Ohashi K, Muramoto A, Shima Y, et al. Differential activities, subcellular distribution and tissue expression patterns of three members of Slingshot family phosphatases that dephosphorylate cofilin. Genes to cells : devoted to molecular & cellular mechanisms. 2003; 8:811–24. [PubMed: 14531860]

93. Oleinik NV, Krupenko NI, Krupenko SA. ALDH1L1 inhibits cell motility via dephosphorylation of cofilin by PP1 and PP2A. Oncogene. 2010; 29:6233–44. [PubMed: 20729910]

94. Gohla A, Birkenfeld J, Bokoch GM. Chronophin, a novel HAD-type serine protein phosphatase, regulates cofilin-dependent actin dynamics. Nature cell biology. 2005; 7:21–9.

95. Huang TY, DerMardirossian C, Bokoch GM. Cofilin phosphatases and regulation of actin dynamics. Current opinion in cell biology. 2006; 18:26–31. [PubMed: 16337782]

96. Lee JH, Palaia T, Ragolia L. Impaired insulin-stimulated myosin phosphatase Rho-interacting protein signaling in diabetic Goto-Kakizaki vascular smooth muscle cells. American journal of physiology Cell physiology. 2012; 302:C1371–81. [PubMed: 22322972]

97. Estey MP, Di Ciano-Oliveira C, Froese CD, Fung KY, Steels JD, Litchfield DW, et al. Mitotic regulation of SEPT9 protein by cyclin-dependent kinase 1 (Cdk1) and Pin1 protein is important for the completion of cytokinesis. The Journal of biological chemistry. 2013; 288:30075–86. [PubMed: 23990466]

Biological significance

These results identify a large number of potential new substrates of serine/threonine protein phosphatase 1 and suggest that serine/threonine protein phosphatase 1 regulatory subunit 12A indeed plays a regulatory role in multiple pathways related to insulin action, providing novel insights into the biology of skeletal muscle insulin signaling. This information may facilitate the design of experiments to better understand the molecular mechanism responsible for skeletal muscle insulin resistance and associated diseases, such as type 2 diabetes and cardiovascular diseases.

Highlights

- Created a PPP1R12A knockdown L6 cell line and identified 620 novel phosphosites
- PPP1R12A knockdown resulted in significantly changed phosphorylation of 698 sites
- PPP1R12A knockdown led to significantly impacted insulin signaling pathways
- Provides novel insights into PPP1R12A's role in skeletal muscle insulin signaling

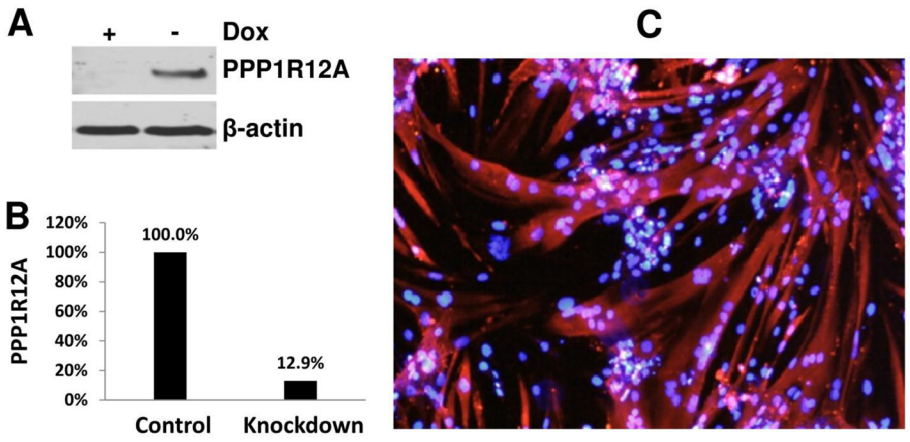

Fig. 1. Characterization of the L6K76 cell line

A. L6K76 cells were treated with or without Dox for 3 days. Cell lysates (120 μg each) were resolved by 4–15% SDS-PAGE. Western blotting was carried out using PPP1R12A and β-actin antibodies. B. PPP1R12A protein level was quantified from Western blot bands normalized to the β-actin level. C. L6K76 cells differentiated into myotubes after induction. Confluent L6K76 cells were induced in DMEM containing 2% FBS for 8 days. The fixed cells were immunostained with mouse monoclonal anti-MyHC (red). Nuclei were counterstained with DAPI (blue).

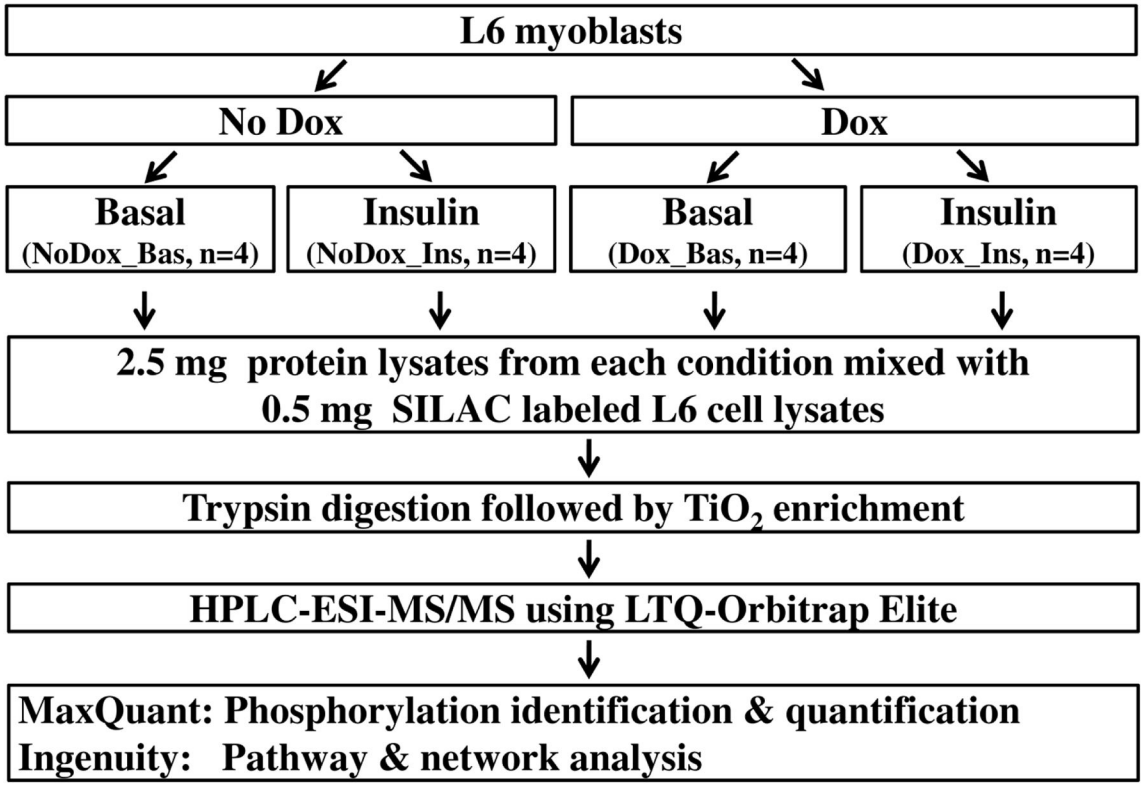

Figure 2A

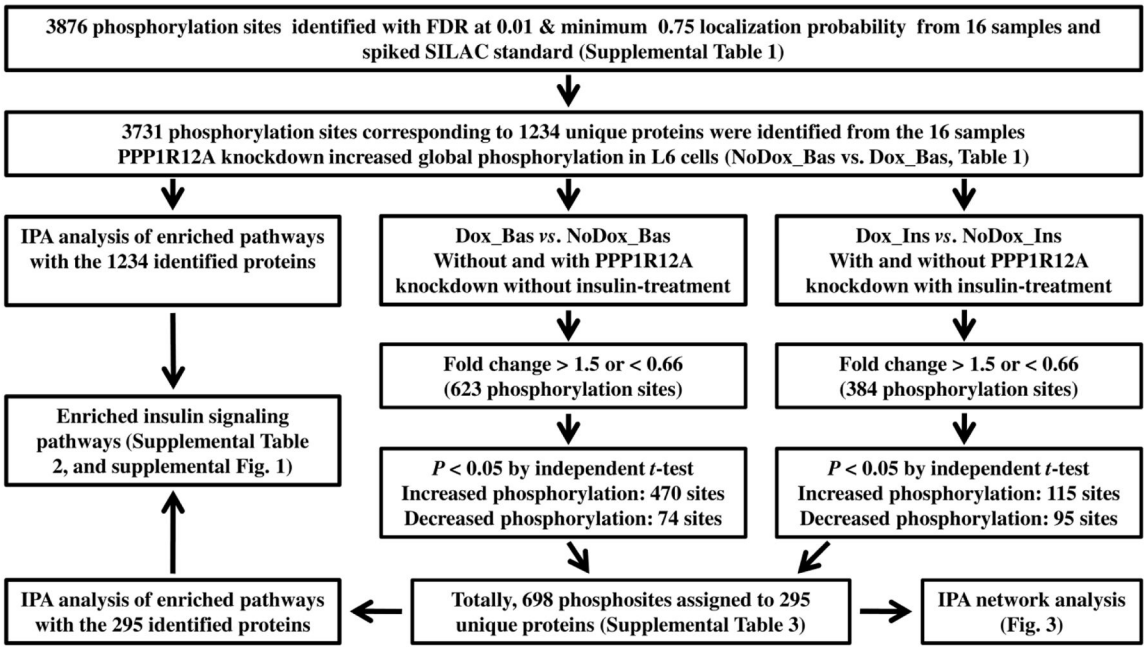

Figure 2B

Fig. 2.

Flow-chart of phosphoproteomics data acquisition and data analysis.

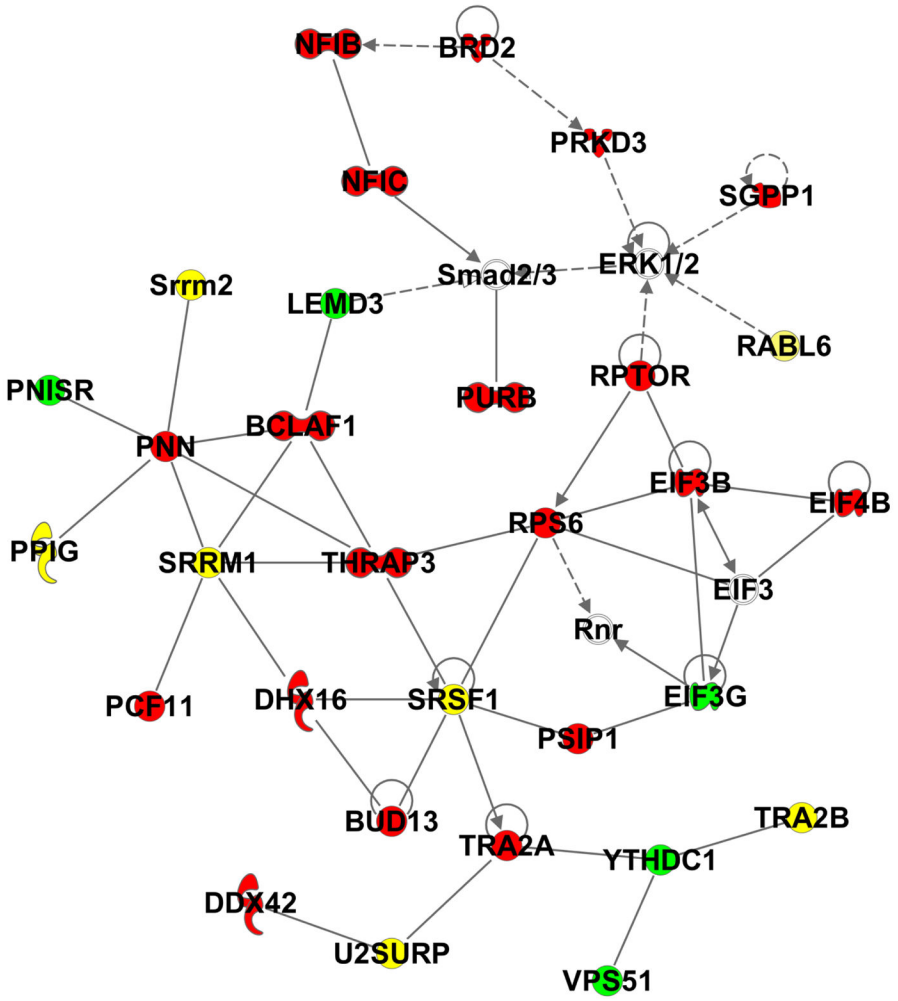

Fig. 3. The highest scored network obtained by IPA for proteins with altered phosphorylation after PPP1R12A knock-down

Proteins with increased phosphorylation site (s) are highlighted in red. Proteins with decreased phosphorylation site (s) are highlighted in green. Proteins with both increased and decreased site (s) are highlighted in yellow. Proteins without color are the ones in the network in the IPA database, but were not identified in this study. Solid and dashed connecting lines indicate the presence of direct and indirect interactions, respectively.

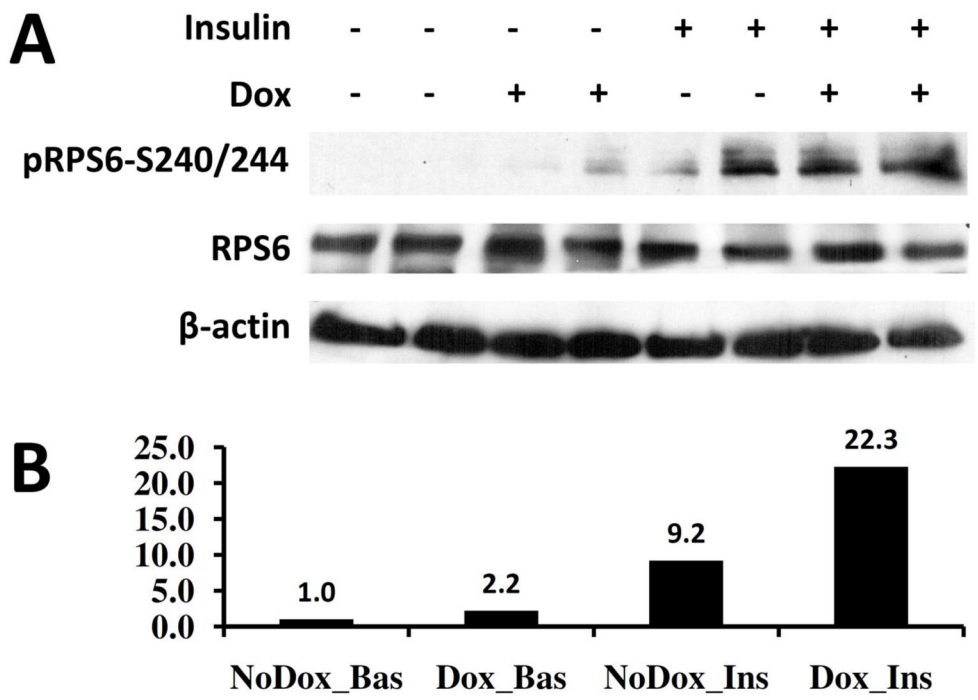

Fig. 4. PPP1R12A knockdown led to increased RPS6 phosphorylation at site S240/244

PPP1R12A knockdown was achieved by maintaining L6K76 myoblasts in media containing 100 ng/ml Dox for three days. Insulin stimulation was carried out by subjecting cells in 100 nM insulin for 15 min. (A). The RPS6 phosphorylation levels at site S240/244 were analyzed by Western blot. (B). Using ImageJ, RPS6 phosphorylation at S240/244 was quantified from Western blot bands normalized to the RPS6 total protein level. The average phosphorylation level of NoDox_Bas group was set as 1.

Table 1

PPP1R12A knockdown increased global phosphorylation in L6 cells at the basal condition.

Group	Dox_Bas	NoDox_Bas	Dox_Ins	NoDox_Ins
I_L/I_u	12.38 ±0.70*	9.76 ± 0.75	11.49 ± 0.91	10.88 ± 0.33

*$P < 0.01$ comparing with NoDox_Bas (cells without PPP1R12A knockdown and without the insulin treatment).

I_u: The total peak area of isotope-labeled phosphopeptides identified in all the sixteen samples (“Universal Standard”).

I_L: the total peak area of all non-labeled phosphopeptides.

Table 2

Phosphorylation changes of proteins identified in pathways related to insulin signaling.

Gene	Protein ID	Protein name	Site	Basal state	Insulin state	Signaling pathway										
				Fold change compared to NoDox_Bas (Dox_Bas vs. NoDox_Bas)	Fold Change compared to NoDox_Ins (Dox_Ins vs. NoDox_Ins)	Insulin receptor	RhoA	mTOR	ERK/MAPK	Phospholipase C	Protein Kinase A	p70S6K	Regulation of eIF4 and p70S6K	T2D	14-3-3-mediated	AMPK
Add1[&]	Q63028	ADDA	T614	1.64[*]	1.24						Y[£]					
Ahnak	M0R9D5	AHNAK	S178	1.96[*]	1.00					Y						
Ahnak	M0R9D5	AHNAK	S213	1.31	0.21[**]					Y						
Ahnak	M0R9D5	AHNAK	S4597	0.40[**]	0.46					Y						
Ahnak	M0R9D5	AHNAK	S5219	3.45[**]	0.99					Y						
Ahnak	M0R9D5	AHNAK	S5225	1.84[*]	0.57					Y						
Ahnak	M0R9D5	AHNAK	S5226	2.04[*]	1.49					Y						
Ahnak	M0R9D5	AHNAK	S5229	2.22[**]	1.12					Y						
Ahnak	M0R9D5	AHNAK	S5232	2.25[**]	1.12					Y						
Ahnak	M0R9D5	AHNAK	S5270	2.77[**]	2.36[**]					Y						
Ahnak	M0R9D5	AHNAK	T5274	2.99[*]	2.58[**]					Y						
Akap1	D4A9M6	AKAP1	S101	3.05[*]	0.46						Y					
Akap8	Q63014	AKAP8	S321	1.43	2.04[*]						Y					
Akap8	Q63014	AKAP8	S326	1.42	1.90[*]						Y					
Akap13	F1M3G7	AKAP13	S1891	>1.50[*#]	NA						Y					
Akt1s1	D3ZH75	PRAS40	T247	0.00	0.33[*]			Y							Y	
Akt1s1	D3ZH75	PRAS40	S88	1.73[*]	0.85			Y							Y	
Arhgap5	Q6TUE6	RhoGAP5	S1173	1.97[**]	1.23		Y									
Arhgap5	Q6TUE6	RhoGAP5	S1176	1.73[**]	1.26		Y									
Arhgef11	Q9ES67	ARHGEF11	S671	1.93[*]	0.37[*]		Y			Y						

Gene	Protein ID	Protein name	Site	Basal state	Insulin state	Signaling pathway										
				Fold change compared to NoDox_Bas (Dox_Bas vs. NoDox_Bas)	Fold Change compared to NoDox_Ins (Dox_Ins vs. NoDox_Ins)	Insulin receptor	RhoA	mTOR	ERK/MAPK	Phospholipase C	Protein Kinase A	p70S6K	Regulation of eIF4 and p70S6K	T2D	14-3-3-mediated	AMPK
Arhgef11	Q9ES67	ARHGEF11	T676	1.93*	0.37		Y			Y						
Cdc23	F1LRQ6	APC8	S588	4.18*	3.00						Y					
Cdc23	F1LRQ6	APC8	T596	4.18*	3.00						Y					
Cdc42ep4	B1WC33	BORG4	S136	3.26*	2.39		Y									
Cdc42ep4	B1WC33	BORG4	S140	3.26*	2.39		Y									
Cfl1	P45592	Cofilin-1	S3	2.93	3.26*		Y									
Eif3b	Q4G061	eIF-3B	S75	1.53*	0.89			Y					Y			
Eif3b	Q4G061	eIF-3B	S79	1.54*	0.92			Y					Y			
Eif3g	Q5RK09	eIF-3G	T41	0.05*	0.33*			Y					Y			
Eif4b	Q5RKG9	eIF-4B	S425	0.31	3.87*			Y								
Flna	C0JPT7	FLN1	S1084	1.72**	1.21						Y					
Hist1h1b	D3ZBN0	H1F5	S2	1.59**	0.30						Y					
Hist1h1d	P15865	H1F3	S2	1.63	0.43*						Y					
Hspb1&	G3V913	HSP27	S200	>1.50**#	3.08				Y							
Hspb1&	G3V913	HSP27	S203	>1.50**#	3.08				Y							
Irs1^	G3V7V7	IRS1	S522	1.42	3.02*	Y						Y	Y	Y		Y
Map3k7	P0C8E4	TAK1	S439	1.86*	1.42									Y		
Mprip&	G3V9F3	MRIP	S294	1.75**	2.24		Y			Y						
Pln	P61016	PLN	S16	2.74*	0.97						Y					
Pln	P61016	PLN	T17	2.74*	1.03						Y					
Ppp1r12a	D3ZR53	PPP1R12A	S507	0.21	0.17**	Y	Y		Y	Y	Y					
Prkd3	D4A229	PKD3	S213	3.50*	1.05			Y		Y	Y	Y		Y	Y	

Gene	Protein ID	Protein name	Site	Basal state	Insulin state	Signaling pathway										
				Fold change compared to NoDox_Bas (Dox_Bas vs. NoDox_Bas)	Fold Change compared to NoDox_Ins (Dox_Ins vs. NoDox_Ins)	Insulin receptor	RhoA	mTOR	ERK/MAPK	Phospholipase C	Protein Kinase A	p70S6K	Regulation of eIF4 and p70S6K	T2D	14-3-3-mediated	AMPK
Prkd3	D4A229	PKD3	S216	3.50*	1.05			Y		Y	Y	Y		Y	Y	
Rps6	P62755	RPS6	S235	3.24	1.73**			Y				Y	Y			
Rps6	P62755	RPS6	S236	1.85*	1.62			Y				Y	Y			
Rps6	P62755	RPS6	S240	2.68**	2.07			Y				Y	Y			
Rps6	P62755	RPS6	S244	2.12**	3.15**			Y				Y	Y			
Rps6	P62755	RPS6	S247	4.28	>1.50*$			Y				Y	Y			
Rptor	D3ZDU2	raptor	S859	5.59**	1.36	Y		Y								Y
Rptor	D3ZDU2	raptor	S863	2.83**	1.04	Y		Y								Y
Sept9	F1LN75	septin 9	S12	1.97**	1.88**		Y									
Sept9	F1LN75	Septin 9	T24	>1.50**#	NA		Y									
Src	G3V776	c-Src	Y419	0.92	2.96*				Y	Y		Y			Y	Y

*:$P < 0.05$.

**: $P < 0.01$.

#: Not detected in samples of NoDox_Bas, while detected in at least three samples of Dox_Bas.

$: Not detected in samples of NoDox_Ins, while detected in at least three samples of Dox_Ins.

£: indicated a protein is assigned to the pathway.

&Reported PPP1R12A interaction partners in reference [11]

^Reported PPP1R12A interaction partners in reference [19].